ELSEVIER

Catalysis Today 39 (1997) 159–168

CATALYSIS TODAY

Design of photocatalysts encapsulated within the zeolite framework and cavities for the decomposition of NO into N_2 and O_2 at normal temperature

Masakazu Anpo*, Shu Guo Zhang, Hirotsugu Mishima, Masaya Matsuoka, Hiromi Yamashita

Department of Applied Chemistry, College of Engineering, Osaka Prefecture University, Gakuen-cho 1-1, Sakai, Osaka 599, Japan

Abstract

The design of photocatalysts encapsulated within the zeolite frameworks and cavities is the most promising approach in developing photocatalysts which will operate efficiently and effectively towards the purification of toxic agents such as NO_x and SO_x in the atmosphere. In the present study, the vanadium silicalite (VS-2) and Ag^+/ZSM-5 catalysts were prepared by hydrothermal synthesis and ion-exchange, respectively, and the in situ characterization of these catalysts and their photocatalytic reactivities for the decomposition of NO have been investigated using dynamic photoluminescence, XAFS (XANES, EXAFS), ESR, FT–IR, UV–VIS, solid-state NMR and XRD techniques along with an analysis of the reaction products. Results obtained with the VS-2 catalyst showed that vanadium oxide moieties are present within the zeolite framework as a 4-fold tetrahedrally coordinated vanadium oxide species having a terminal oxovanadium group (V=O). UV irradiation of the VS-2 catalyst in the presence of NO led to the photocatalytic decomposition of NO to form N_2, N_2O and O_2. On the other hand, it was found that the zeolite cavities can stabilize the Ag^+ ions in an isolated state through their connection with two lattice oxygen anions of the zeolite (2-coordination geometry). These isolated Ag^+ ions exhibit high photocatalytic reactivities for NO decomposition to form N_2, N_2O and NO_2. Dynamic studies of the excited state of these catalysts showed that the charge transfer from the excited state of the vanadium oxide species or Ag^+ ions to NO plays a vital role in the initiation of the decomposition of NO into N and O. These findings have demonstrated that metal oxide species and metal ions included within the zeolite frameworks and cavities are strong candidates for new types of environmentally applicable photocatalysts.

Keywords: Photocatalysis; Vanadium silicalite; Ag^+/ZSM-5; NO_x decomposition

1. Introduction

A great deal of attention has been directed towards various useful applications of photocatalysts for achieving our better environment and although this field has expanded rapidly with regard to light energy, especially the conversion of solar energy into useful chemical energy using solid photocatalysts such as TiO_2 [1–12], more recently, the application of photocatalysis to reduce toxic agents in the atmosphere and water [13–18], especially NOx, as well as CO_2 and SOx in the atmosphere has become urgent [19,20].

Ammoxidiation on the V_2O_5/TiO_2 catalyst has been developed as a de-NO_x-ing process [21]. However, strongly desired are catalytic systems for the direct

*Corresponding author.

0920-5861/97/$32.00
PII S0920-5861(97)00097-7

decomposition of NO_x which operate at ambient temperatures and ambient pressure conditions without the use of NH_3. The direct decomposition of NO into N_2 and O_2 on ion-exchanged Cu^+/ZSM-5 zeolite catalysts have been investigated at around 600–800 K [22]. Furthermore, utilizing photocatalytic processes in gas–solid systems can be said to be one of the most promising approaches in dissolving and reducing environmental toxins.

The unique and fascinating properties of zeolites involving transition metals within the zeolite frameworks or cavities have opened new possibilities in many research areas not only for catalysis but also for various photochemical processes [23–28]. The transition metal ions in metalosilicate zeolites are expected to be highly dispersed at an atomic level and considered to be well-defined catalysts, which are included within the specific structure of the zeolite frameworks [23,24,29–31]. The Löwenstein rule stipulates that Al atoms within the zeolite frameworks cannot connect directly with each other [32]. If this can be applied to metalosilicate zeolites, well-prepared zeolite samples should contain only isolated metal ions. This is of great significance in the design of highly dispersed transition metal oxide catalysts, such as V, Mo, or Ti-oxides, which are well known in that their highly dispersed states can induce unique photocatalytic reactivities and selectivities [13]. On the other hand, the countercations within the zeolite cavities can very easily be exchanged by different cations through a conventional ion-exchange method [25–28]. Since the ion-exchangeable sites are well separated from each other within the cavities, ion-exchange with metal ions having photocatalytic properties are an attractive approach in preparation of efficient and effective photocatalysts. In addition to these effects, the higher surface area of zeolites and their unique micropore structures also exhibit a condensation effect on the dilute toxic gasses involving a micro-filling effect [29]. Only a meticulous characterization of the specific properties and effects of both the metal oxides or metal cations encapsulated within the zeolite frameworks and cavities at the molecular level will facilitate the design of useful photocatalysts.

In this article, we will present our recent work on the photocatalytic decomposition of NO on the vanadium silicalite (VS-2) and Ag^+/ZSM-5 photocatalysts prepared in the zeolite framework and cavities, respectively. Dynamic photoluminescence, XAFS (XANES, EXAFS), ESR, FT–IR, UV–VIS, solid-state wide-line ^{51}V-NMR and XRD techniques have been applied for a detailed characterization of the local structure of the active species or sites to examine the relationship between the local structure of the active sites and their photocatalytic properties as well as to clarify the reaction mechanisms at the molecular level.

2. Utilization of vanadium silicalite as a photocatalyst for the direct decomposition of NO

Zeolites having transition metal cations in their frameworks have been given considerable attention for their interesting and distinctive catalytic properties [23,24,30,31]. Titanium silicalites exhibit a unique catalytic reactivity in the oxidation reactions of alkanes and aromatics with H_2O_2 as an oxidizing agent while the titanium oxide species in the zeolite framework play a vital role as the active sites [23,24]. Several XAFS investigations have revealed that the titanium oxide species included within the zeolite framework exist in an isolated state, having a tetrahedral coordination, and the unique catalytic properties observed can be attributed to the unique local structure of the titanium oxide species [30,31].

Although several types of vanadium silicalite catalysts in which vanadium ions are incorporated in the zeolite framework have recently been developed [33–35], the true chemical nature and reactivities of the vanadium silicalites are yet little known, especially their photochemical properties [36]. According to our previous work, vanadium oxide highly dispersed on silica shows unique photocatalytic properties towards the partial oxidation of alkenes as well as other notable reactions [37–41]. In this case, the dispersion level is the key factor in controlling the photocatalytic properties. A well-prepared vanadium silicalite contains uniform vanadium oxide moieties in its framework and can exhibit unique photocatalytic reactions.

Along these lines, in the following section, the distinct characteristics of the vanadium oxide species anchored in the zeolite framework and their reaction with gaseous NO at 298 K under UV irradiation will be reviewed at the molecular level using various in situ spectroscopic techniques.

2.1. *Preparation and characterization of the vanadium silicalite catalyst*

Vanadium silicalite (VS-2) catalysts were hydrothermally synthesized and modified in accordance with the procedures published previously [34,35], using tetraethylorthosilicate (TEOS) as the silicon sources and $VCl_3 \cdot nH_2O$ or $VOSO_4 \cdot nH_2O$ as the vanadium sources. Tetrabutylammonium hydroxide (TBAOH) was used as a template. The Si/M ratio of the catalysts as determined by chemical analysis was 50–150. Prior to spectroscopic measurements and photocatalytic reactions, the catalyst was degassed at 725 K, heated in O_2 at the same temperature and then finally evacuated at the desired temperature.

The results of XRD analysis indicate that the resulting zeolites have a silicalite-2 structure and the extent of crystallization is high. IR spectral investigations showed significant bands at 960–970 cm^{-1}, indicating the successful incorporation of vanadium ions into the zeolite framework.

The shape of the XANES spectra provides direct and useful information on the local structure and coordination geometry of the central vanadium atoms [42]. Fig. 1 shows the XAFS spectra of the treated VS-2 catalyst and the reference $VO(O\text{-}i\text{-}C_3H_7)_3$ compounds recorded at 295 K. The characteristic feature of both XANES spectra is the appearance of a preedge peak due to the so-called 1s-3d transition which is mainly caused by the mixing of 2p orbitals of the oxygen molecules with 3dp orbitals of the vanadium atoms. This p–d mixing suggests the presence of a terminal oxovanadium group (V=O) [42]. It was also found that the shape of the XANES spectrum of the VS-2 catalyst is quite similar to that of the $VO(O\text{-}i\text{-}C_3H_7)_3$ complex indicating that the VS-2 catalyst consists of vanadium oxide species having a tetrahedral coordination in C_{3v} symmetry.

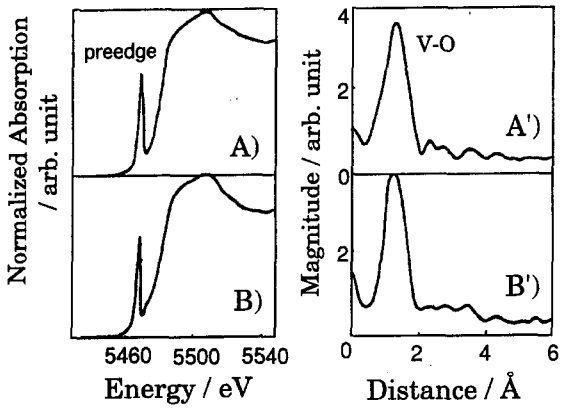

Fig. 1. The XANES spectra (A, B) and FT-EXAFS spectra (A′, B′) of the evacuated VS-2 catalyst (A, A′) and those of $VO(O\text{-}i\text{-}Pr)_3$ (B, B′).

Furthermore, in the FT-EXAFS spectrum, only a single peak due to the presence of neighboring oxygen atoms (V–O) can be observed at about 1.4 Å (without phase-shift correction) revealing that vanadium ions are highly dispersed in the VS-2 catalyst. In the curve fitting analysis of the XAFS spectrum, the best fitting was obtained with one oxygen in the shorter V–O distance of 1.64 Å and three oxygen atoms in the long V–O distance of 1.73 Å. Furthermore, in addition to these results, the EXAFS spectra recorded at 77 K provide the evidence of the presence of another oxygen atom located at the longer distance of 2.21 Å, indicating the presence of the weak interaction of the vanadium species with the neighboring surface OH groups of the zeolite.

In the solid-state wide-line ^{51}V-NMR spectra, the reference V_2O_5 exhibited a single band at −290 ppm while the hydrated VS-2 catalyst exhibited a band at around −530 ppm, having a small shoulder at around −590 ppm. Upon evacuation at 475 K this band shifted to −640 ppm. According to previous NMR studies on the highly dispersed vanadium oxide species [43,44], the peaks at around −530 ppm are attributed to the presence of distorted T_d-like coordinated vanadium oxide species while the C_{3v}-like coordinated vanadium oxide species exhibit a peak in the region of −600∼−700 ppm. The evacuated VS-2 catalyst exhibited only one peak at around −640 ppm, suggesting that the vanadium oxide species is present in tetrahedral coordination and not in octahedral coordination. The absence of signals at around −290 ppm indicates that the VS-2 catalyst is completely free of the V_2O_5 compound. This shows a good agreement with the C_{3v} model defined in the XAFS studies.

The ESR technique was also applied to investigate the local structure of the vanadium oxide species included within the zeolite framework by monitoring the V^{4+} ions which were produced by the photoreduction of the catalyst with H_2 at 77 K. The photoreduc-

tion at 77 K was so mild that no local structural rearrangement around the surface vanadium ions occurred [40,41]. Two sets (signal A with $g_{\|}$=1.880 and $g_{\perp}$=1.991; signal B with $g_{\|}$=1.937 and $g_{\perp}$=1.991) of 8-equally spaced lines due to the I=7/2 spin of the V atoms and centered on $g_z=g_{xx}$ can clearly be seen. The addition of a small amount of water onto the catalyst caused signal A to disappear completely and only signal B remained. The ESR parameters of signal A were in good agreement with those of V^{4+} ions located in tetrahedral coordination while signal B showed good agreement with ions in octahedral coordination. A good correspondence with the results obtained with the VZSM-12 catalyst can be seen [45].

From these results obtained by XAFS, NMR and ESR measurements, it seems clear that the treated VS-2 catalyst has a C_{3v} symmetrical metal center in a tetrahedral coordination.

2.2. *Excited state of the V-silicalite-2 catalyst and its interaction with NO*

As shown in Fig. 2, the VS-2 catalyst evacuated at 475 K exhibits a photoluminescence spectrum at around 450–550 nm with a well-resolved vibrational fine structure upon excitation of the absorption (excitation) band at around 270–340 nm (Fig. 2(B)). These absorption (excitation) and photoluminescence spectra are in good agreement with those obtained with well-defined highly dispersed vanadium oxides anchored on Vycor glass or silica and can be attributed to the following charge transfer processes on the surface vanadyl groups of the tetrahedral vanadium oxide species, involving an electron transfer from O^{2-} to V^{5+} and a reverse radiative decay [37–41].

$$(V^{5+}=O^{2-}) \underset{h\nu'}{\overset{h\nu}{\rightleftarrows}} (V^{4+} - O^{-})^*$$

The photoluminescence spectrum scarcely changed when the excitation wavelengths were changed and decayed as a beautiful single exponential suggesting that only one kind of vanadium oxide species is present in the catalyst and responsible for the photoluminescence spectrum. The lifetime was determined to be about 6.9 ms at 77 K and 0.1 ms at 295 K, respectively. These values were found to be comparative but slightly shorter than those of the highly dispersed vanadium oxides anchored on Vycor glass or silica. These photoluminescence data obtained with the VS-2 catalyst provide sufficient evidence to suggest the presence of a tetrahedral VO_4 unit structure within the zeolite framework which corresponded with results obtained by XAFS, NMR and ESR studies.

Fig. 2 also shows the second-derivative photoluminescence spectrum obtained at 77 K (Fig. 2(E)). The spectrum indicates that the energy separation between the (0→0) and (0→1) transition bands is about 956 cm^{-1} and can be attributed to the vibronic transition in the V=O bond. An energy separation of 956 cm^{-1} obtained from the hyperfine structure of the photoluminescence spectrum of the VS-2 catalyst was found to be slightly different from that of the vanadium oxide species highly dispersed on Vycor glass or silica (1035 cm^{-1}) [40,41], therefore, indicating the presence of some perturbation due to the neighboring surface OH groups in the electronic state of the V=O species included in the zeolite framework. The presence of this weak interaction could be observed only by an analysis of the hyperfine structure of the photoluminescence spectrum at 77 K. These results lead us to conclude that the model shown in Fig. 3 can be proposed as the local structure of the VS-2 catalyst.

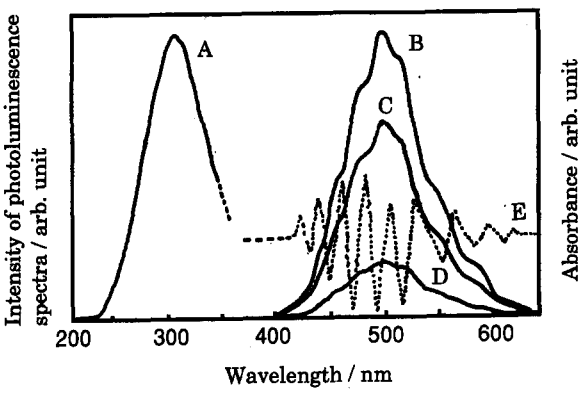

Fig. 2. The photoluminescence spectrum and its excitation spectrum of the evacuated VS-2 catalyst at 77 K and the effect of the addition of NO on the photoluminescence of the VS-2 catalyst. (A) Excitation spectrum; (B) photoluminescence spectrum and the quenching by the addition of NO with (C) 0.06 Torr and (D) 0.4 Torr; (E) the second derivative spectrum of photoluminescence spectrum (B).

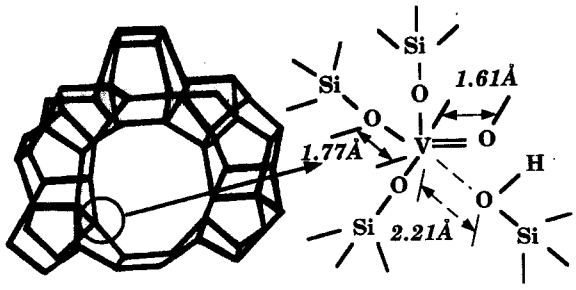

Fig. 3. The proposed local structure of vanadium oxide moieties in the VS-2 catalyst.

As also shown in Fig. 2, the addition of NO onto the VS-2 catalyst led to an efficient quenching of the photoluminescence both in its yield and lifetime. The Stern-Volmer plots for the quenching of the photoluminescence by the addition of NO at 295 K showed an excellent linearity, indicating that the excited state of the vanadium oxide species in the VS-2 catalyst interacts with the added NO. These results indicate that the tetrahedral VO_4 moieties in C_{3v} symmetry can be expected to exhibit photocatalytic properties.

2.3. *Photocatalytic decomposition of NO on the V-silicalite-2 catalyst*

The direct photocatalytic decomposition of NO into N_2 was carried out in a quartz reactor under UV-irradiation at 295 K using a high pressure mercury lamp through water and color filters. UV irradiation (λ>280 nm) of the VS-2 catalyst at 295 K in the presence of NO led to the formation of N_2, O_2 and N_2O. The reaction time profiles for the formation of N_2 are shown in Fig. 4. The formation of N_2 is found only under irradiation and the yields increase with a good linearity against the UV irradiation time. After prolonged irradiation, the turnover frequency defined by the number of N_2 produced, divided by the number of total number of V atoms included within the catalyst, exceeded 1.0, indicating that the reaction proceeds photocatalytically on the VS-2 catalyst even at 295 K.

The ESR signals were obtained by the addition of NO pressure onto the VS-2 catalyst. The ESR signal due to the adsorbed NO disappeared easily by the evacuation of the system, indicating that the interaction of NO with the catalyst is weak and NO is

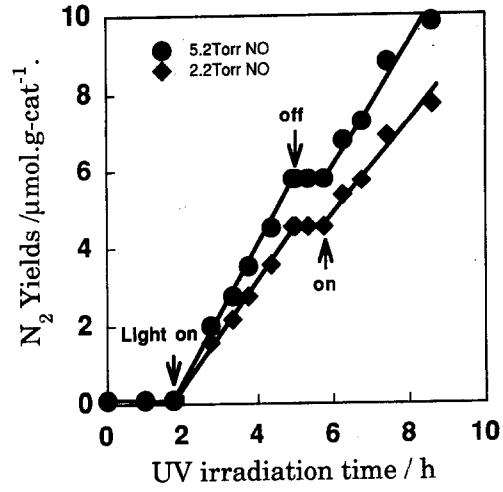

Fig. 4. The time profile of the photocatalytic decomposition of NO into N_2 on the VS-2 catalyst at 295 K.

physically adsorbed on the catalyst. UV irradiation of the catalyst having the adsorbed NO species led to a decrease in the intensity of the ESR signal. After UV irradiation was discontinued, the intensity of the signal returned to its original level. This sensitive response of the ESR signal towards UV irradiation suggests that the adsorbed NO species plays a role as a precursor of the photocatalytic reaction. In fact, as shown in Fig. 4, the pressure dependence of NO on the yields of the photocatalytic decomposition of NO, i.e., the higher the NO pressure, the faster the reaction rate is found, suggests that the adsorbed NO surface species play a vital role in the photoreaction.

Taking the photoreactivity of the V=O species of the tetrahedrally coordinated vanadium oxides into account, the following reaction scheme may be proposed for the direct photo-induced decomposition of NO into N_2 and O_2. On the vanadium oxide species having a V=O band, two NO species are adsorbed as weak ligands to form the reaction precursor species. Under UV irradiation the charge transfer excited complexes, $(V^{4+}\text{–}O^{-})^{*}$ are formed. Within their lifetimes the electron transfer from the electron trapped center (V^{4+}) into the π^{*}-antibonding orbital of NO takes place and simultaneously the electron transfer from the π-bonding orbital of another NO into the hole trapped center (O^{-}) occurs. These electron transfer processes lead to the direct decomposition of the two NO species into N_2 and O_2 under UV irradiation even

at 295 K. Understanding the significance such local charge separation play in photocatalytic reactions at the molecular level will contribute to the development of new and efficient photocatalytic systems.

3. Utilization of the Ag^+/ZSM-5 as photocatalyst for the direct decomposition of NO

The unique physicochemical properties of zeolites such as shape selective pore structures of molecular scale and ion exchange capacities allow the anchoring of various metal cations within the zeolite cavities by a combination of ion-exchange and thermovacuum treatments [25–27]. Recently, we have reported that UV irradiation of Cu^+ ions anchored onto silica or zeolites leads to the electronic excitation of Cu^+ ions from the d^{10} ground state to the d^9s^1 electronic excited state as shown in the following scheme [25–27]:

$$Cu^+([Ar]3d^{10}) \xrightarrow{h\nu} Cu^{+*}([Ar]3d^9 4s^1)$$

With these catalysts, under UV irradiation both the s electron and the d hole are produced on the Cu^+ ions which behave as the localized charge separation state. As a result, the anchored Cu^+ ions can initiate unique photocatalytic properties which cannot be realized on semiconductor-type photocatalysts. Especially, the Cu^+/ZSM-5 catalyst can decompose NO into N_2 and O_2 photocatalytically with high selectivity, and the photochemically excited state of the isolated Cu^+ ions are considered to play a significant role in this reaction [25–27]. However, the preparation of the Cu^+/ZSM-5 catalyst requires evacuation at temperatures higher than 975 K to produce Cu^+ ions as the active species and in the presence of O_2 or under the high pressure of NO, the oxidation of Cu^+ ions to Cu^{2+} ions easily occurs leading to the deactivation of the catalyst.

The Ag^+ ion which has the same electronic configuration as the Cu^+ ion (d^{10}) as well as the advantage of being chemically stable in an oxidative atmosphere can act as an efficient photocatalyst for the decomposition of NO diluted in air. Moreover, ion-exchanged silver/zeolite catalysts have been reported to show very high activity for the disproportionation of ethylbenzene [46,47], the photochemical and/or thermal cleavage of water to H_2 and O_2 [48], photo-induced oxygen production from water [49], photo-induced dimerization of alkanes [50], as well as the selective reduction of NO by ethylene at around 825 K [51] or by ethanol at around 725 K [52].

The following section will examine the characteristics of the Ag^+ species anchored in the nano-pores of the ZSM-5 zeolite and their reaction with gaseous NO at 295 K under UV irradiation at the molecular level by in situ photoluminescence, ESR, XAFS and UV–VIS measurements [53–55].

3.1. *Preparation and characterization of the Ag^+/ZSM-5 catalyst*

The Ag^+/ZSM-5 (SiO_2/Al_2O_3=23.3) sample was prepared by ion-exchange with an aqueous $Ag(NH_3)_2^+$ solution. After washing with water and drying in air at 375 K, the silver loading of the sample was determined to be 6.7 wt% as metal. Prior to spectroscopic and photocatalytic measurements, the samples were degassed at 295 K for 1 h, calcined at 675 K in the presence of 20 Torr of O_2 for 1 h, then degassed at 475 K for 1 h.

Fig. 5 shows the FT-EXAFS spectra of the Ag^+/ZSM-5 catalyst (A′), bulk Ag_2O (B′) and Ag foil (C′),

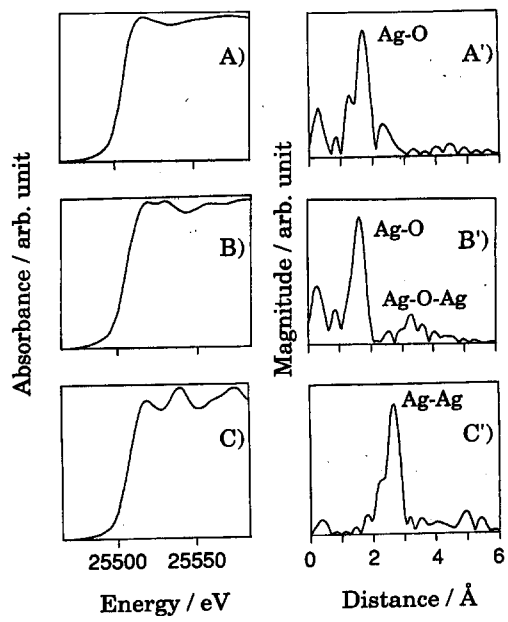

Fig. 5. The XANES spectra (A–C) and FT-EXAFS spectra (A′–C′) of the Ag^+/ZSM-5 catalyst (A, A′), Ag_2O powder (B, B′) and Ag foil (C, C′).

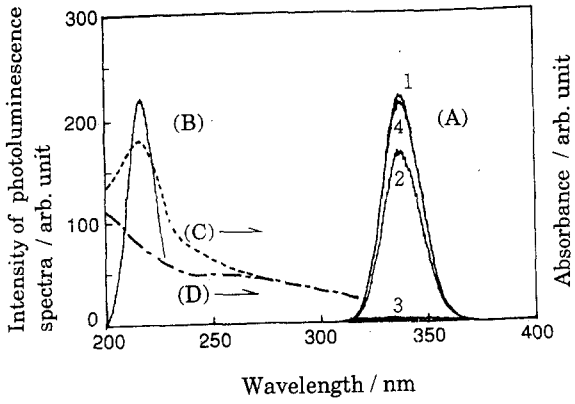

Fig. 6. The photoluminescence spectra (A) and its excitation spectrum (B) of the Ag^+/ZSM-5 catalyst, the effect of the addition of NO on the photoluminescence (2–4) and the absorption spectrum of the Ag^+/ZSM-5 (dotted line: C) and H^+/ZSM-5 catalysts measured by UV diffuse reflectance method (dashed line: D) (The addition of NO was carried out at 295 K. NO pressure (in Torr): 1, 0.0; 2, 0.2; 3, 4.0: 4, after the degassing of NO at 295 K.) (The excitation spectra were monitored at 342 nm emission.).

respectively. The FT-EXAFS spectrum of Ag_2O (B′) exhibits a peak at around 3.5 Å which can be attributed to the Ag–O–Ag bonding, and the FT-EXAFS of the Ag foil (C′) exhibits a peak at around 2.5 Å due to the Ag–Ag bonding (phase shift has not been corrected). However the FT-EXAFS of the Ag^+/ZSM-5 catalyst exhibits a well-defined peak attributed to the neighboring oxygen atoms (Ag–O) only at around 1.8 Å. This suggests that silver is anchored within the micropores of the ZSM-5 zeolite in an isolated state forming neither clusters nor Ag metal or oxide crystals.

As shown in Fig. 6(C), the Ag^+/ZSM-5 catalyst exhibits an intense absorption band at around 220 nm which is attributed to the $4d^{10}\rightarrow 4d^9 5s^1$ electronic transition of the Ag^+ ions [56–58]. While, the H^+/ZSM-5 exhibited no intense absorption band in the 200–250 nm wavelength range (Fig. 6(D)). The Ag^0 atoms, and Ag_n^0 and Ag_m^{n+} clusters are known to exhibit absorption bands at wavelengths above 250 nm [59,60]. However, no absorption band of the Ag^+/ZSM-5 appeared in this region. Furthermore, no EPR signals assigned to the Ag^0 atoms or Ag^{2+} species were observed with the Ag^+/ZSM-5 catalyst. These results firmly support the conclusion that silver ions are included within the pore structure of the ZSM-5 zeolite as isolated Ag^+ ions.

3.2. *Excited state of the Ag^+/ZSM-5 catalyst and its interaction with NO*

An ESR signal was obtained at 77 K after the addition of 7 Torr of NO onto the Ag^+/ZSM-5 catalyst at 295 K. The appearance of the hyperfine splitting of the signal shows that the paramagnetic electron interacts with the nucleus of Ag^+ (I=1/2) suggesting that the NO are adsorbed on the Ag^+ to form a nitrosylic adduct, i.e., Ag^+–$NO^{\delta-}$ as has been detected on the Cu^+/ZSM-5 catalyst [61]. The evacuation of the system led to the disappearance of the signal indicating that the interaction of NO with the Ag^+ ion is weak. UV irradiation of the Ag^+/ZSM-5 catalyst having the Ag^+–$NO^{\delta-}$ species led to a decrease in the intensity of the ESR signal assigned to the Ag^+– $NO^{\delta-}$ species in correspondence with the UV irradiation time and without the appearance of any new signal. After UV irradiation was discontinued, the intensity of the signal returned to its original level. These reversible changes in the ESR signal attributed to Ag^+–$NO^{\delta-}$ species suggest not only that the Ag^+–$NO^{\delta-}$ species act as reaction precursors but also that the photo-induced decomposition of NO proceeds catalytically.

Fig. 6 shows the photoluminescence spectrum (A) and its corresponding excitation spectrum (B) of the Ag^+/ZSM-5 catalyst. The excitation band at around 220 nm shows a good coincidence with the absorption band which is attributed to the electronic transition, i.e., $4d^{10}\rightarrow 4d^9 5s^1$ of the isolated Ag^+ ion on the Ag^+/ZSM–5 catalyst. The excitation band at around 220 nm and photoluminescence band at around 340 nm can be attributed to the presence of the isolated Ag^+ ion, i.e., the electronic excitation of $4d^{10}\rightarrow 4d^9 5s^1$ and its reverse radiative deactivation process of $4d^9 5s^1\rightarrow 4d^{10}$, respectively, as shown in the following scheme:

$$Ag^+([Kr]4d^{10}) \underset{h\nu'}{\overset{h\nu}{\rightleftarrows}} Ag^{+*}([Kr]4d^9 5s^1)$$

Fig. 6 also shows the effect of the addition of NO on the photoluminescence spectrum of the Ag^+/ZSM-5 catalyst. The addition of NO onto the catalyst leads to the efficient quenching of the photoluminescence due to the isolated Ag^+ ion (Fig. 6; 2–3). After complete quenching, the evacuation of the system leads to recovery of the photoluminescence to its original

intensity (Fig. 6; 4). These results clearly indicate that the interaction of NO with the Ag^+ ion is weak, and that the added NO easily interacts with the Ag^+ species in its ground as well as excited states. The photoluminescence of the Ag^+/ZSM-5 catalyst was more easily quenched by the addition of NO than that of the Cu^+/ZSM-5 catalyst suggesting that in its electronically excited states Ag^+ ions interact with NO more efficiently than Cu^+ ions.

3.3. *Photocatalytic decomposition of NO on the Ag^+/ZSM-5 catalyst*

Photocatalytic reactions were carried out at 295 K using a high pressure mercury lamp and water filter. UV irradiation of the Ag^+/ZSM-5 catalyst in the presence of 10 Torr of NO at 295 K was found to lead to the formation of N_2, N_2O and NO_2. The reaction profiles for the formation of N_2 and N_2O are shown in Fig. 7. The formation of N_2 and N_2O can be found only under UV irradiation and the yield of these products increases with a good linearity against the irradiation time, suggesting that the reaction proceeds photocatalytically. On the H^+/ZSM-5 catalyst and the Ag^0/ZSM-5 catalyst prepared by heating

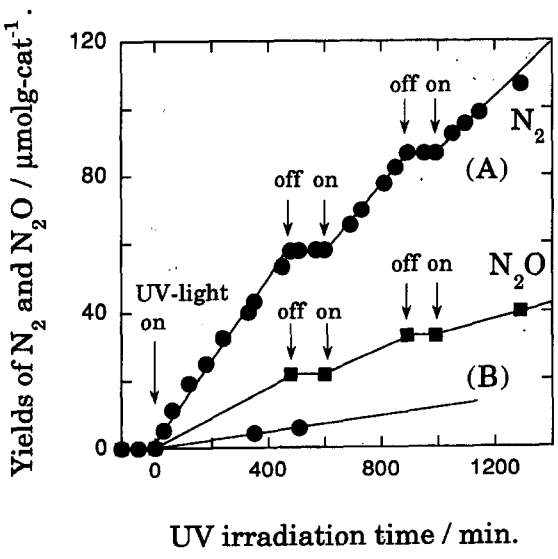

Fig. 7. The time profiles of the photocatalytic decomposition of NO into N_2 and N_2O on the Ag^+/ZSM-5 catalyst (A) and Cu^+/ZSM-5 catalyst (B) at 295 K.

Ag^+/ZSM-5 with H_2, the formation of minor amounts of N_2 and N_2O was observed, but was found to be small and negligible compared to the yield of the reaction for the UV irradiated Ag^+/ZSM-5 catalyst. These results clearly demonstrate that the Ag^+ ions of the catalyst play a significant role in the photocatalytic decomposition of NO.

Fig. 7 also shows that the rate of N_2 formation on the Ag^+/ZSM-5 catalyst is 10 times faster than on the Cu^+/ZSM-5 catalyst [25], indicating that the photocatalytic decomposition of NO proceeds faster on the Ag^+ ions than on the Cu^+ ions. As for the reaction products, N_2, N_2O, and NO_2 were produced, suggesting that the decomposition of NO on the Ag^+/ZSM-5 catalyst proceeds in a distinctly different way from the reaction of NO on the Cu^+/ZSM-5 catalyst to produce N_2 and O_2 (though the formation of NO_2 was also found on the Cu^+/ZSM-5 when the UV irradiation was carried out at the higher pressure of NO). Under UV irradiation of the catalyst through the UV-25 filter (>250 nm), the photocatalytic decomposition of NO proceeded at 15% the rate without the UV cut filter, i.e., with the full arc of the high pressure mercury lamp. This indicates that the UV light effective for NO decomposition lies in the wavelength regions of 200–250 nm.

The most effective wavelength of UV light for the photocatalytic decomposition of NO (200~250 nm) lies in the same wavelength region as the absorption band and excitation band of Ag^+/ZSM-5 which are attributed to the presence of the Ag^+ ions (220 nm). These results clearly indicate that the electronic excited state of the Ag^+ ions is directly associated with the photocatalytic decomposition of NO. As mentioned above, since Ag^0/ZSM-5 did not show any photocatalytic activity for the decomposition of NO, it can be concluded that the Ag_n^0 or Ag_m^{n+} clusters are not associated with the reaction.

The effects of the addition of O_2 and H_2O on the yield of the photocatalytic decomposition reaction of NO were also investigated on the Cu^+/ZSM-5 and Ag^+/ZSM-5 catalysts. The coexistence of O_2 with the reactant NO greatly deactivated the Cu^+/ZSM-5 catalyst, however, in the case of the Ag^+/ZSM-5 catalyst, the reactivity was maintained in spite of a decrease in the reaction yield. It is clear that the Ag^+ ions are stable even in an oxidative atmosphere while the Cu^+ ions are easily oxidized into the Cu^{2+} ions. Under the

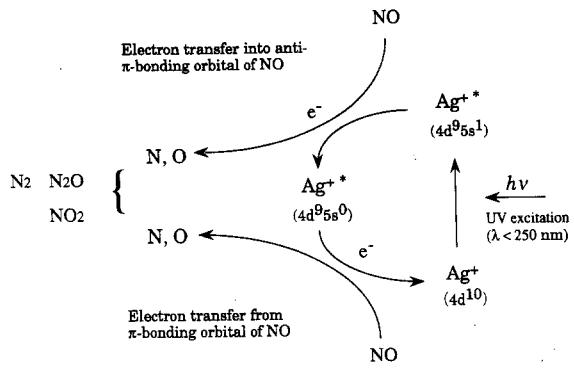

Fig. 8. Reaction scheme of the photocatalytic decomposition of NO on the Ag^+/ZSM-5 catalyst at 295 K.

coexistence of 20% of H_2O, 90% of the reactivity of the Ag^+/ZSM-5 catalyst is maintained as compared to that without H_2O. These results indicate that the Ag^+/ZSM-5 catalyst can act as an efficient photocatalyst for the decomposition of NO diluted in air.

From these various findings, as can be seen in Fig. 8, it could be concluded that the electronically excited state of highly dispersed isolated Ag^+ ions ($4d^95s^1$) is directly associated with the photocatalytic decomposition of NO: an electron transfer from the excited state of Ag^+ ion into the π^*-antibonding molecular orbital of NO initiates the weakening of the N–O bond and at the same time an electron transfer from the π-bonding orbital of another NO to the vacant orbital of the Ag^+ ion leads to the weakening of the N–O bond, resulting in the formation of N_2, N_2O, and NO_2. The remarkably high photocatalytic reactivity of the Ag^+/ZSM-5 catalyst can be attributed to the high chemical stability of the Ag^+ ions and the efficient interaction of the electronically excited state of the Ag^+ ions with NO as compared with the Cu^+ ions on the Cu^+/ZSM-5 catalyst.

4. Conclusions

In this article, a detailed characterization of the vanadium oxide species introduced into the silicalite framework and the Ag^+ ions exchanged onto the ZSM-5 zeolite, the interaction of NO with these catalysts as well as the photocatalytic decomposition of NO have been described at the molecular level. It was found that the design of photocatalysts with metal oxides or cations encapsulated within the zeolite framework and cavities is an effective approach in obtaining efficient and unique photocatalysts which enable the direct decomposition of NO. The vanadium oxide species can be effectively dispersed in a tetrahedral coordination by introducing them into the zeolite framework. The charge transfer excited state of the tetrahedrally coordinated V–O moieties having a terminal oxovanadium group (V=O) plays a vital role as active sites for the photocatalytic decomposition of NO on the VS-2 catalyst. Furthermore, the cavities of the zeolites are able to stabilize the exchanged transition metal cations with lower coordination numbers. These highly dispersed isolated Ag^+ ions within the zeolite cavities show high photocatalytic reactivity for NO decomposition, and the electron transfer between the excited state of the Ag^+ ions and NO is responsible for the activation process of this reaction. These findings have demonstrated that metal oxides and cations included within the zeolite framework or cavities are the most promising candidates for new and unique photocatalysts which will lead to the appearance of more selective and efficient photocatalytic systems

Acknowledgements

The present work has been supported in part by the Grant-in-Aid on Priority-Area-Research on "Photoreaction Dynamics" (06239110), "Catalytic Chemistry of Unique Reaction Fields" (08232271) and International Joint Project Research (07044162) of the Ministry of Education, Science, Sports, and Culture of Japan. M. Anpo is much indebted to Osaka Prefecture for the Special Project Research and Tokyo Ohka Foundation for their financial support, as well as to the Tosoh Corporation for kindly providing the zeolite samples.

References

[1] A. Fujishima, K. Honda, Nature 238 (1972) 37.
[2] A.J. Bard, J. Phys. Chem. 86 (1982) 172.
[3] A. Heller, Science 233 (1984) 1141.
[4] M. Gratzel, Energy Resources through Photochemistry and Catalysis, Academic Press, New York, 1983.
[5] M.A. Fox, Accts. Chem. Res. 16 (1983) 314.

[6] N. Serpone, E. Pelizzetti, Photocatalysis, Wiley, New York, 1988.
[7] E. Pelizzetti, M. Schiavello, Photochemical Conversion and Storage of Solar Energy, Kluwer Academic Publishers, Amsterdam, 1991.
[8] M. Schiavello, Photocatalysis and Environment, Kluwer Academic Publishers, Amsterdam, 1988.
[9] P.V. Kamat, Chem. Rev. 93 (1993) 267.
[10] P. Pichat, Catal. Today 19 (1994) 313.
[11] K. Zamaraev, M.I. Khramov, V.N. Parmon, Catal. Rev. Sci. Eng. 36 (1994) 617.
[12] M. Anpo, T. Matsuura, Photochemistry on Solid Surfaces, Elsevier, Amsterdam, 1989.
[13] Anpo, H. Yamashita, in: M. Anpo (Ed.), Surface Photochemistry, Wiley, West Sussex, 1996, p. 116.
[14] D.F. Ollis, H. Al-Ekabi, Photocatalytic Purification and Treatment of Water and Air, Elsevier, Amsterdam, 1993.
[15] M.A. Fox, M.T. Dulay, Chem. Rev. 93 (1993) 341.
[16] A. Heller, Acc. Chem. Res. 28 (1995) 503.
[17] M.R. Hoffman, S.T. Martin, W. Choi, D.W. Bahnemann, Chem. Rev. 95 (1995) 69.
[18] A.L. Linsebigler, G. Lu, J.T. Yates Jr., Chem. Rev. 95 (1995) 735.
[19] M. Anpo, H. Yamashita, in: M. Schiavello (Ed.), Heterogeneous Photocatalysis, Wiley, West Sussex, 1997, p. 131.
[20] M. Anpo, M. Matsuoka, H. Mishima, H. Yamashita, Res. Chem. Intermed., in press.
[21] H. Bosch, F. Janssen, Catal. Today 2 (1988) 369.
[22] M. Iwamoto, H. Yahiro, N. Mizuno, W.X. Zhang, Y. Mine, H. Furukawa, S. Kagawa, J. Phys. Chem. 96 (1992) 9360.
[23] T. Tatsumi, M. Nakamura, S. Negishi, H. Tominaga, J. Chem. Soc. Chem. Commun. (1990) 476.
[24] J.S. Reddy, R. Kumar, J. Catal. 130 (1991) 440.
[25] M. Anpo, M. Matsuoka, Y. Shioya, H. Yamashita, E. Giamello, C. Morterra, M. Che, H.H. Patterson, S. Webber, S. Ouellette, M.A. Fox, J. Phys. Chem. 98 (1994) 5744.
[26] E. Giamello, D. Murphy, G. Magnacca, C. Morterra, Y. Shioya, T. Nomura, M. Anpo, J. Catal. 136 (1992) 510.
[27] H. Yamashita, M. Matsuoka, K. Tsuji, Y. Shioya, M. Anpo, J. Phys. Chem. 100 (1996) 397.
[28] H. Yamashita, Y. Ichihashi, M. Anpo, V. Louis, M. Che, J. Phys. Chem., in press.
[29] M. Jaroniec, R. Madey, J. Phys. Chem. 92 (1988) 3986.
[30] S. Bordiga, S. Coluccia, C. Lamberti, L. Marchese, A. Zecchina, F. Boscherini, F. Buffa, F. Genoni, G. Leofanti, G. Petrini, G. Vlaic, J. Phys. Chem. 98 (1994) 1253.
[31] T. Blasco, M.A. Camblor, A. Corma, J. Perez-Pariente, J. Am. Chem. Soc. 115 (1993) 11806.
[32] W. Löwenstein, Am. Mineral. 39 (1954) 92.
[33] A. Miyamoto, D. Medhanayn, T. Inui, Appl. Catal. 28 (1986) 89.
[34] P.R. Hari Prasad Rao, A.V. Ramaswamy, P. Ratnasamy, J. Catal. 137 (1992) 225.
[35] T. Inui, D. Medhanavyn, P. Praserthdam, K. Fukuda, T. Ukawa, A. Sakamoto, A. Miyamoto, Appl. Catal. 18 (1985) 311.
[36] M. Anpo, S.G. Zhang, H. Yamashita, Stud. Surf. Sci. Catal. 101 (1996) 941.
[37] M. Anpo, Y. Shioya, M. Che, Res. Chem. Intermed. 17 (1992) 15.
[38] H. Patterson, J. Cheng, M. Sunamoto, M. Anpo, J. Phys. Chem. 95 (1991) 8813.
[39] M. Anpo, I. Tanahashi, Y. Kubokawa, J. Phys. Chem. 84 (1980) 3340.
[40] M. Anpo, M. Sunamoto, T. Fujii, H.H. Patterson, M. Che, Res. Chem. Intermed. 11 (1989) 245.
[41] M. Anpo, M. Sunamoto, M. Che, J. Phys. Chem. 93 (1989) 1187.
[42] T. Tanaka, H. Yamashita, R. Tsuchitani, T. Funabiki, S. Yoshida, J. Chem. Soc., Faraday Trans. 1 84 (1988) 2987.
[43] H. Eckert, I.E. Wachs, J. Phys. Chem. 93 (1989) 6796.
[44] B. Taouk, M. Guelton, J. Grimblot, J.P. Bonnelle, J. Phys. Chem. 92 (1988) 6700.
[45] I.L. Moudrakovski, A. Sayari, C.I. Ratclie, J.A. Ripmeester, K.F. Preston, J. Phys. Chem. 98 (1994) 10895.
[46] T. Baba, Y. Ono, Zeolites 7 (1987) 292.
[47] Y. Ono, T. Baba, K. Kanae, S.G. Seo, J. Chem. Soc. Jpn. 7 (1988) 985.
[48] P.A. Jacobs, J.B. Uytterhoeven, H.K. Beyer, J. Chem. Soc., Chem. Commun. (1977) 128.
[49] G. Calzaferri, S. Hug, T. Hugentobler, B. Sulzberger, J. Photochem. 26 (1984) 109.
[50] G.A. Ozin, F. Hugues, J. Phys. Chem. 86 (1982) 5174.
[51] S. Sato, Y. Yu-u, H. Yahiro, N. Mizuno, M. Iwamoto, Appl. Catal. 70 (1991) L1.
[52] T. Miyadera, A. Abe, G. Muramatsu, K. Yoshida, Proceedings of the Symposium on Envir. Conscious Mater: Third IUMRS International Conference on Adv. Mater., Tokyo, 1993.
[53] M. Matsuoka, E. Matsuda, K. Tsuji, H. Yamashita, M. Anpo, Chem. Lett. (1995) 375.
[54] M. Matsuoka, E. Matsuda, K. Tsuji, H. Yamashita, M. Anpo, J. Mol. Catal. 107 (1996) 399.
[55] M. Anpo, M. Matsuoka, H. Yamashita, Catal. Today 35 (1997) 177.
[56] C.E. Moore, Atomic Energy Levels, Vol. 3, National Bureau of Standards, Washington, DC, 1971, p. 48.
[57] A.N. Truklin, S.S. Etsin, A.V. Shendrik, Izv. Akad. Nauk. SSSR, Ser. Fiz. 40 (1976) 2329.
[58] J. Texter, R. Kellerman, T. Gonsiorwski, J. Phys. Chem. 90 (1986) 2118.
[59] G.A. Ozin, H. Huber, Inorg. Chem. 17 (1978) 155.
[60] G.A. Ozin, F. Hugues, S.M. Matter, D.F. McIntosh, J. Phys. Chem. 87 (1983) 3445.
[61] C. Chao, J.H. Lunsford, J. Phys. Chem. 78 (1974) 1174.